THERMAL STRESS ANALYSIS OF SYMMETRIC SHELLS SUBJECTED TO ASYMMETRIC THERMAL LOADS*

Gordon R. Negaard
ANAMET Laboratories, Incorporated

SUMMARY

This paper presents a study of the performance of the NASTRAN level 16.0 axisymmetric solid elements when subjected to both symmetric and asymmetric thermal loading. A ceramic radome was modeled using both the CTRAPRG and the CTRAPAX elements. The thermal loading applied contained severe gradients through the thickness of the shell. Both elements were found to be more sensitive to the effect of the thermal gradient than to the aspect ratio of the elements. Analysis using the CTRAPAX element predicted much higher thermal stresses than the analysis using the CTRAPRG element, prompting studies of models for which theoretical solutions could be calculated. It was found that the CTRAPRG element solutions were satisfactory, but that the CTRAPAX element was very geometry dependent. This element produced erroneous results if the geometry was allowed to vary from a rectangular cross-section. The most satisfactory solution found for this type of problem was to model a small segment of a symmetric structure with isoparametric solid elements and apply the cyclic symmetry option in NASTRAN.

INTRODUCTION

Two recent studies have been conducted to determine stresses in ceramic radomes due to asymmetric thermal loadings. Transient thermal loads in both studies produced much sharper temperature gradients through the thickness of the shell than along the surface. For this reason, shell elements could not be used and it was necessary to use a formulation capable of modeling a three-dimensional temperature distribution. In the first study, four layers of NASTRAN level 16.0 twenty node isoparametric bricks (CIHEX2) of various thicknesses were used to construct a radome model (Fig. 1). The thermal loading simulated a threat level laser irradiation. The results were found to be very dependent upon matching the nodal spacing to the temperature distribution and a problem size limitation was reached where economics prohibited creating a finer model which would be less sensitive to the temperature gradient.

In the second study, the thermal loading simulated both axisymmetric and non-axisymmetric aerodynamic heating. The structure was modeled with a CTRAPAX axisymmetric element capable of handling both loading cases. The nodal point temperatures for an axisymmetric thermal load case are shown in Figure 2,

---

*The work described herein was performed by the Aerospace Structures Information & Analysis Center (ASIAC) at the Air Force Flight Dynamics Laboratory, WPAFB, Ohio under Air Force Contract F33615-77-C-3046.

which also illustrates the modeling of the radome nose-tip. The grid illustrated represents the third iteration of the mesh size. The initial grid had the same spacing through the thickness but was several times coarser in the axial direction. This resulted in temperature gradients between nodal points of as much as 600°R. The NASTRAN results predicted unrealistically high stresses which were at first thought to be a function of the temperature gradient. The grid shown in Figure 2 reduced these gradients to less than 300°R, however, the stress levels were still not believable. A switch to CTRAPRG elements produced maximum compressive stresses of about 21000 psi, which agreed well with a SAAS III analysis and indicated that the CTRAPAX elements were indeed predicting erroneous stresses. These cases had been conducted with temperature dependent material properties so both elements were run with the temperature dependence removed, however this changed the results only slightly, eliminating this also as a possible source of the error.

At this point, the reason for the variations in the stresses predicted by the two elements were unknown. A preliminary study on a hollow cylinder had shown almost identical answers for both a linearly and logarithmically varying radial temperature distribution for the two elements. Various ways of modeling the radome with triangles and quadrilateral elements were investigated to determine if the problem was a function of modeling techniques. This did not appear to be so since all combinations of the AX elements produced similar stresses and the RG elements likewise produced a set of similar stresses. Figures 3 and 4 compare hoop stresses for the two elements and show that the CTRAPAX element predicts a ridiculously high stress of more then 600,000 psi in the same area. Since only the CTRAPAX and CTRIAAX elements could handle asymmetric loading, it was necessary to determine the reliability of these elements before continuing with the asymmetric aerodynamic heating case.

SYMBOLS

α = thermal expansion coefficient

ν = poisson's ratio

E = young's modulus

T = temperature field

σ = stress

t = thickness

b = radius

DISC ANALYSIS

In order to determine why the CTRAPAX and CTRAPRG elements produced differing results for the radome model, a simple disc model restrained at the outer circumference and which had known theoretical solutions was chosen (ref. 1). Both a quadratically varying radial temperature and a linearly varying axial temperature could be applied as shown in Table 1. The model and cross-sections of the axisymmetric model using rectangular elements are shown in Figure 7. For this model, both types of elements produced exact theoretical answers for aspect ratios varying from 1.0 to 10.0 for temperature independent material properties for combinations of radially and axially varying temperatures. This eliminated aspect ratios and two-dimensional temperature gradients as being responsible for the differing results in the radome. There was no theoretical solution for temperature dependent material properties, however, both elements still produced identical answers. This left geometry of the elements as the only likely remaining candidate for the source of error.

The geometry of the elements was changed so that all elements had at least one skewed side instead of being rectangular (Fig. 7). This model was then run with only the radially varying temperature distribution. These runs produced results that definitely proved that the CTRAPAX elements produced incorrect results when a non-rectangular cross-section is used. For the temperature independent results, the CTRAPRG elements produced results which matched the theoretical solution exactly, while the CTRAPAX elements gave radial and hoop stresses sixty to one hundred per cent too high. Even worse, these elements predicted axial stresses almost as high as the axial and radial stresses while the CTRAPRG results agreed with the theoretical solution of zero stress. The temperature dependent material runs predicted stresses that followed the same pattern but of course could not be compared to a theoretical solution. These results are shown in Figures 8 through 11.

This analysis showed that the CTRAPRG element appeared to produce reliable results while confirming that the CTRAPAX element could not be trusted in a model requiring the use of non-rectangular element shapes, essentially ruling out the use of the CTRAPAX element in a model simulating a radome shape. Since only the CTRAPAX and CTRIAAX elements can be used for axisymmetric models subjected to non-axisymmetric loads, it was necessary to look for an alternate way of solving the asymmetric aerodynamic heating problem.

RING ANALYSIS

The cyclic symmetry option in NASTRAN was examined to determine if better results for symmetric structures subjected to an asymmetric thermal load could be obtained. A ring subjected to a temperature distribution of the form $T=T_o\ (R^K)\cos(n\theta)$ was chosen because theoretical solutions could be obtained (ref.2). The model of the ring is shown in Figure 12. Both thirty degree and ten degree wedge shapes were examined, requiring twelve and thirty-six cases respectively when running cyclic symmetry. The model cross-section was deliberately made as similar to the previous disc analysis as possible

including the use of skewed elements shapes exactly as used in the previous section. Table 2 describes the formulation of the temperatures used as input and the resulting hoop and radial stresses to be expected. The axial stress should be identically zero. The actual stresses obtained at several radii are shown in Tables 3 and 4 for both ten and thirty degree wedges with skewed and non-skewed geometry. It can be seen that skewness had little effect except for the radial stress in the outermost elements in the ten degree wedge. The axial stresses tended to be less than ten percent of the lower of the radial or hoop stress except at the outer fiber. It was discovered that the axial stresses could be made smaller by making the ring thinner, thus approaching a state of plane stress more closely. Selected plots of hoop stress are shown as Figures 13, 14 and 15. It can be seen in these figures that as the wedge becomes narrower, it appears to approach the theoretical solution as a limit.

CONCLUDING REMARKS

In order to make a comparison of the computer costs of cyclic symmetry against the use of the axisymmetric elements, a ring model with the same geometry using the CTRAPAX elements with non-skewed geometry and temperature input at every fifteen degrees as shown in Table 1 was examined. This produced almost exact theoretical answers, remembering that the CTRAPAX element required that the element shapes be rectangular while the cyclic symmetry option did not have this limitation. The following is a comparison of the running time on the CDC CYBER 74, using level 16.0 NASTRAN with 32 elements in each model.

	CYCLIC SYMMETRY TECHNIQUE		AXISYMMETRIC TECHNIQUE
	(30° Wedge)	(10° Wedge)	(15° Increments)
CM(octal)	165,000	170,000	250,000
CP(sec)	445	1,200	2,681
IO(sec)	333	869	307

These results indicate that the cyclic symmetry option in NASTRAN is better suited to the solution of a general axisymmetric problem under asymmetric loading than the axisymmetric technique. A practical upper limit to the size problem that can be solved with cyclic symmetry remains to be determined.

REFERENCES

1. Wang, C. T., "Applied Elasticity," McGraw-Hill Book Company, Inc., 1953.

2. Maddux, G. E., "Thermo-Structural Analysis Manual," Report No. WADD-TR-60-517, Vol. 1, August, 1962.

TABLE 1. PARAMETERS USED IN DISC MODEL

DISC PROPERTIES

b (OUTER RADIUS = 10.0 INCHES

t (THICKNESS) MAX = 0.4 INCH

t (THICKNESS) MIN = 0.04 INCH

$E = 10^7$ PSI

$\upsilon = \frac{1}{3}$

$\alpha = 10^{-6}$ IN/IN/°R

RADIAL TEMPERATURE AND STRESS VARIATION

$$T(r) = To + (Ti - To)\left[1 - \frac{r^2}{b^2}\right]$$

$$\sigma_{rr}(r) = -\frac{1}{4} E \alpha (Ti - To)\left[\frac{3-\upsilon}{1-\upsilon} - \frac{r^2}{b^2}\right]$$

$$\sigma_{\theta\theta}(r) = -\frac{1}{4} E \alpha (Ti - To)\left[\frac{3-\upsilon}{1-\upsilon} - \frac{3r^2}{b^2}\right]$$

$$\sigma_{zz}(r) = 0$$

AXIAL TEMPERATURE AND STRESS VARIATION

$$T(z) = 1000\,z$$

$$\sigma_{rr}(z) = \sigma_{\theta\theta}(z) = \frac{E \alpha T(z)}{2(1-\upsilon)}$$

$$\sigma_{zz}(z) = 0$$

TABLE 2. PARAMETERS USED IN RING MODEL

RING PROPERTIES

b (OUTER RADIUS) = 1.0 INCH

a (INNER RADIUS) = 0.2 INCH

t (THICKNESS) = 0.08 INCH

$E = 10^7$ PSI

$\upsilon = \frac{1}{3}$

$\alpha = 10^{-6}$ IN/IN/°R

TEMPERATURE AND STRESS VARIATION

$$T(r,\theta) = To\,(\frac{r}{b})^2 \cos\theta$$

$$\sigma_{rr}(r,\theta) = E\,\alpha\,To\,B_k \cos\theta$$

$$\sigma_{\theta\theta}(r,\theta) = E\,\alpha\,To\,D_k \cos\theta$$

r	B_k	D_k
.2	0.0	.1202
.3	.03258	.1177
.4	.04408	.1163
.5	.04808	.1024
.6	.04696	.07364
.7	.04144	.02929
.8	.03170	−.03088
.9	.01788	−.1070
1.0	0.0	−.1990

TABLE 3. STRESSES IN 30° WEDGE MODEL AS A FUNCTION OF ANGLE AND RADIUS

RADIUS (INCHES)	THETA (DEGREES)	RING WITH UNSKEWED ELEMENTS			RING WITH SKEWED ELEMENTS		
		RADIAL	HOOP	AXIAL	RADIAL	HOOP	AXIAL
.25	0	41	187	-4	42	187	-3
	30.0	35	162	-4	36	162	-2
	60.0	20	93	-2	21	94	-2
	90.0	0	0	0	0	0	0
.55	0	87	158	8	87	158	9
	30.0	76	137	7	76	137	8
	60.0	43	79	4	44	79	5
	90.0	0	0	0	0	0	0
.95	0	26	-221	43	26	-221	43
	30.0	23	-192	37	22	-192	37
	60.0	13	-111	22	13	-111	21
	90.0	0	0	0	0	0	0

TABLE 4. STRESSES IN 10° WEDGE MODEL AS A FUNCTION OF ANGLE AND RADIUS

RADIUS (INCHES)	THETA (DEGREES)	RING WITH UNSKEWED ELEMENTS			RING WITH SKEWED ELEMENTS		
		RADIAL	HOOP	AXIAL	RADIAL	HOOP	AXIAL
.25	0	46	224	-8	50	224	-5
	30	40	194	-7	43	194	-5
	60	23	112	-4	25	112	-3
	90	0	0	0	0	0	0
.55	0	101	178	0	102	180	2
	30	87	154	0	89	156	1
	60	50	89	0	51	90	1
	90	0	0	0	0	0	0
.95	0	28	-276	33	18	-279	33
	30	25	-239	28	16	-242	29
	60	14	-138	16	9	-140	17
	90	0	0	0	0	0	0

FIGURE 1. TYPICAL AXISYMMETRIC RADOME MODEL WITH ASYMMETRIC HEAT LOAD

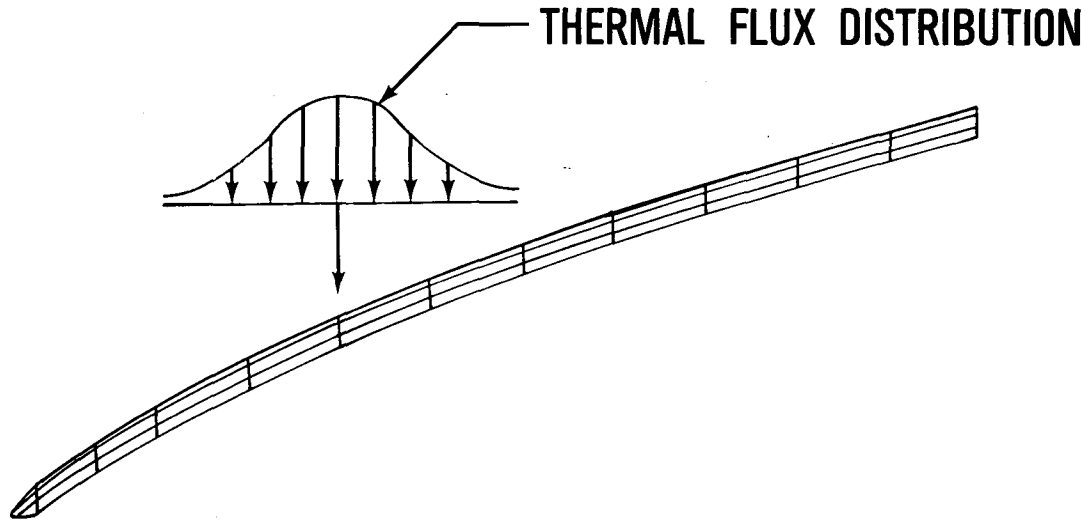

FIGURE 2. NODAL POINT TEMPERATURES, °R, FOR AXISYMMETRIC AERODYNAMIC HEATING

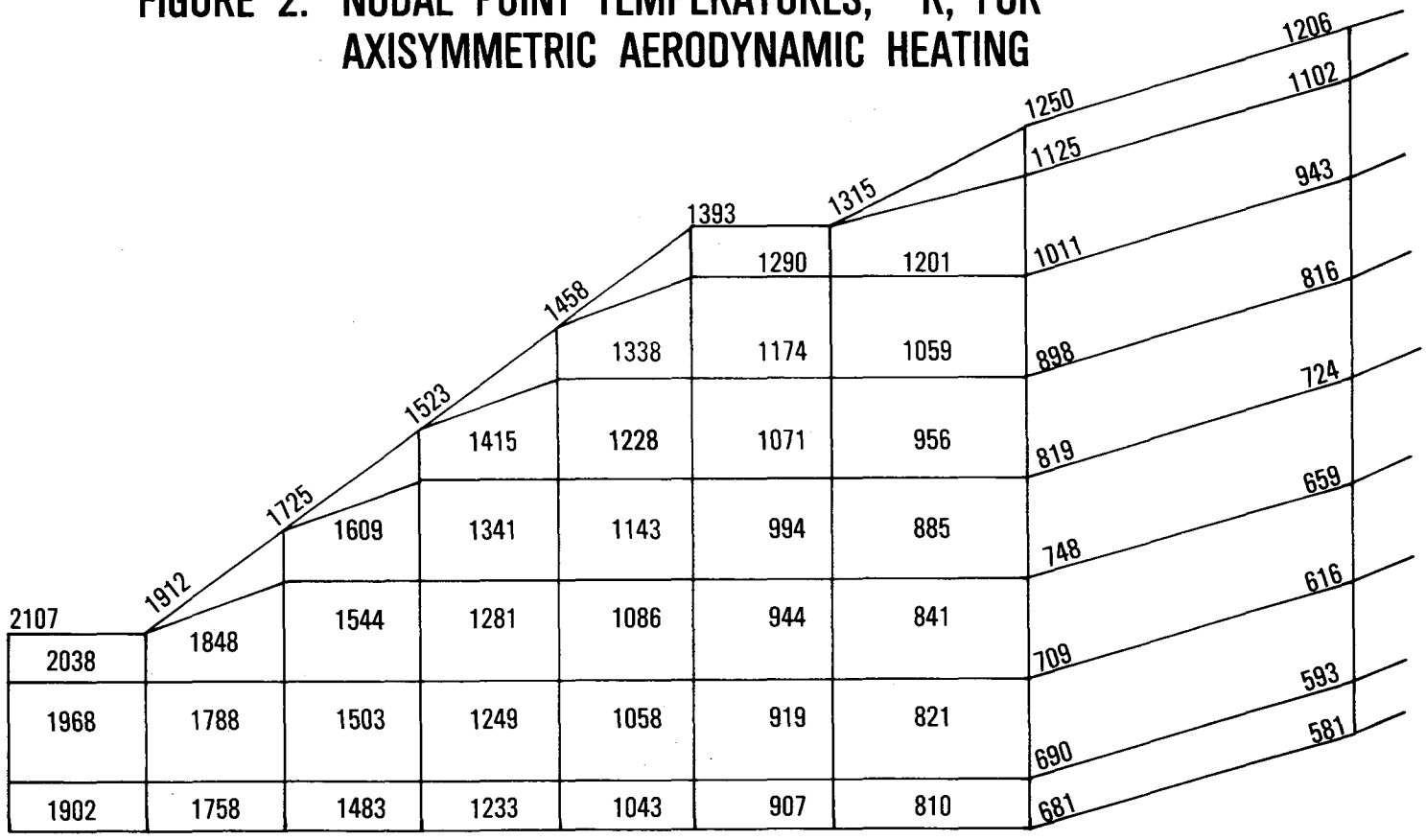

FIGURE 3. HOOP STRESS (PSI) FOR CTRAPAX ELEMENT

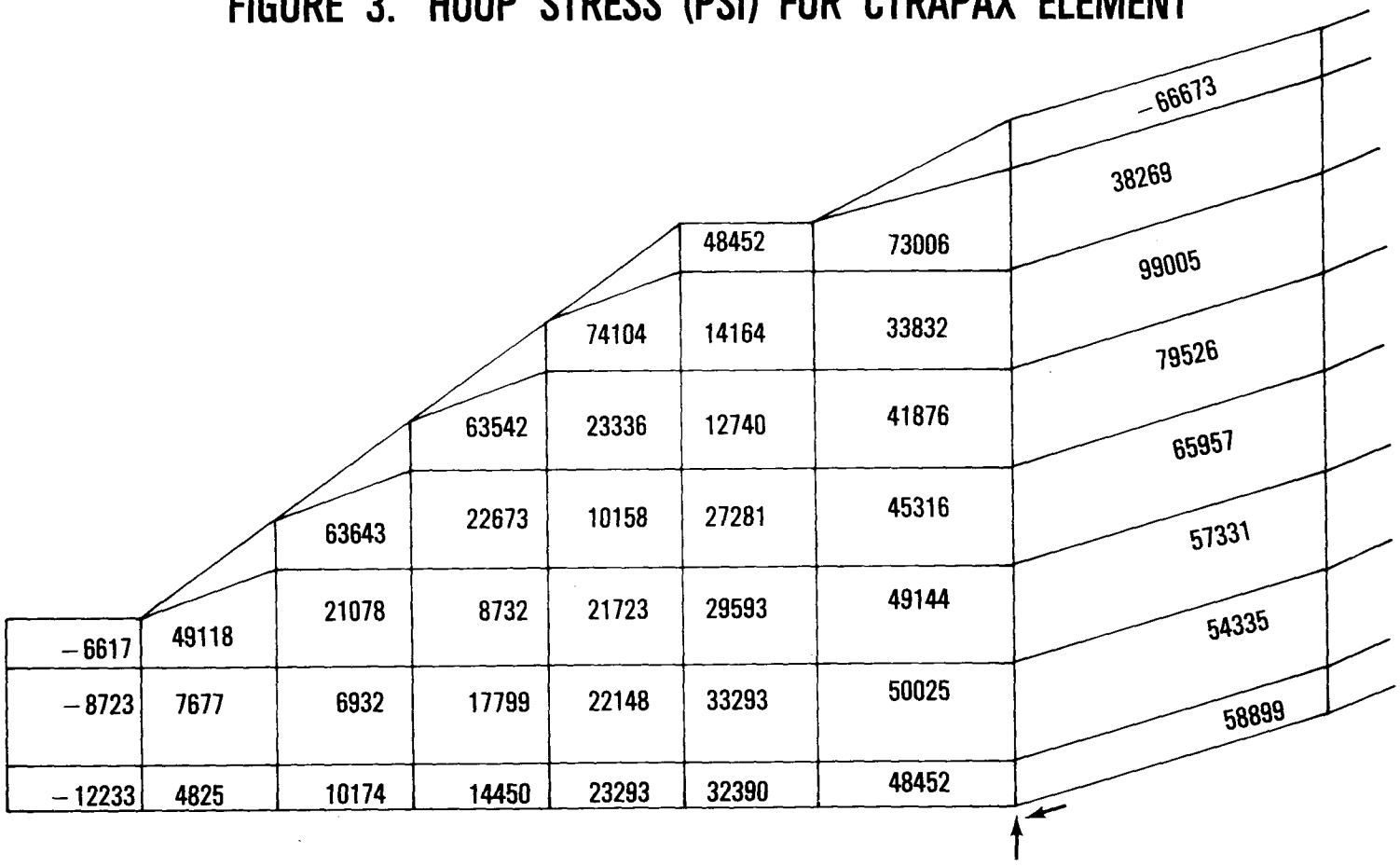

FIGURE 4. HOOP STRESS (PSI) FOR CTRAPRG ELEMENTS

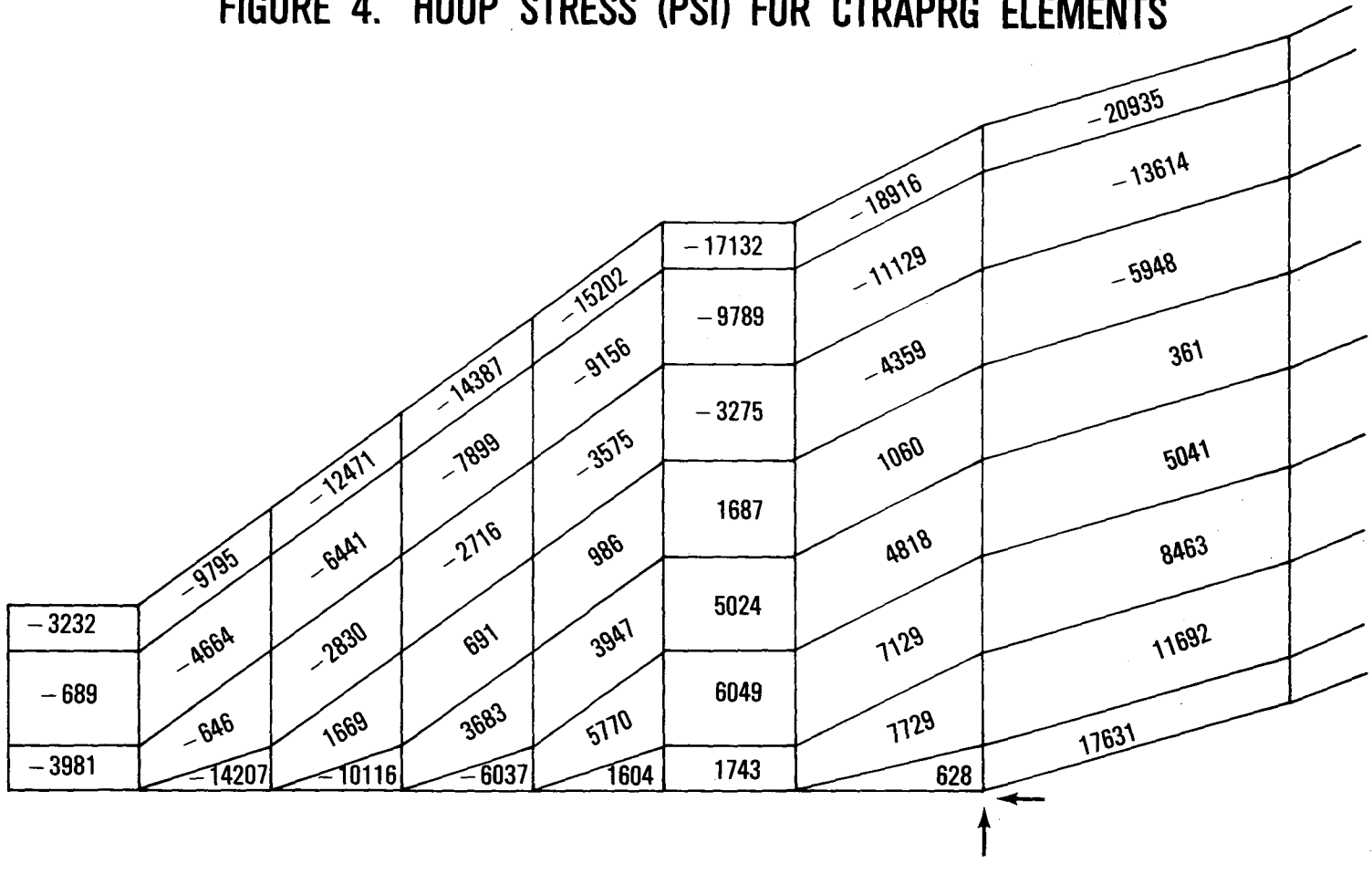

FIGURE 5. AXIAL STRESS (PSI) FOR CTRAPAX ELEMENTS

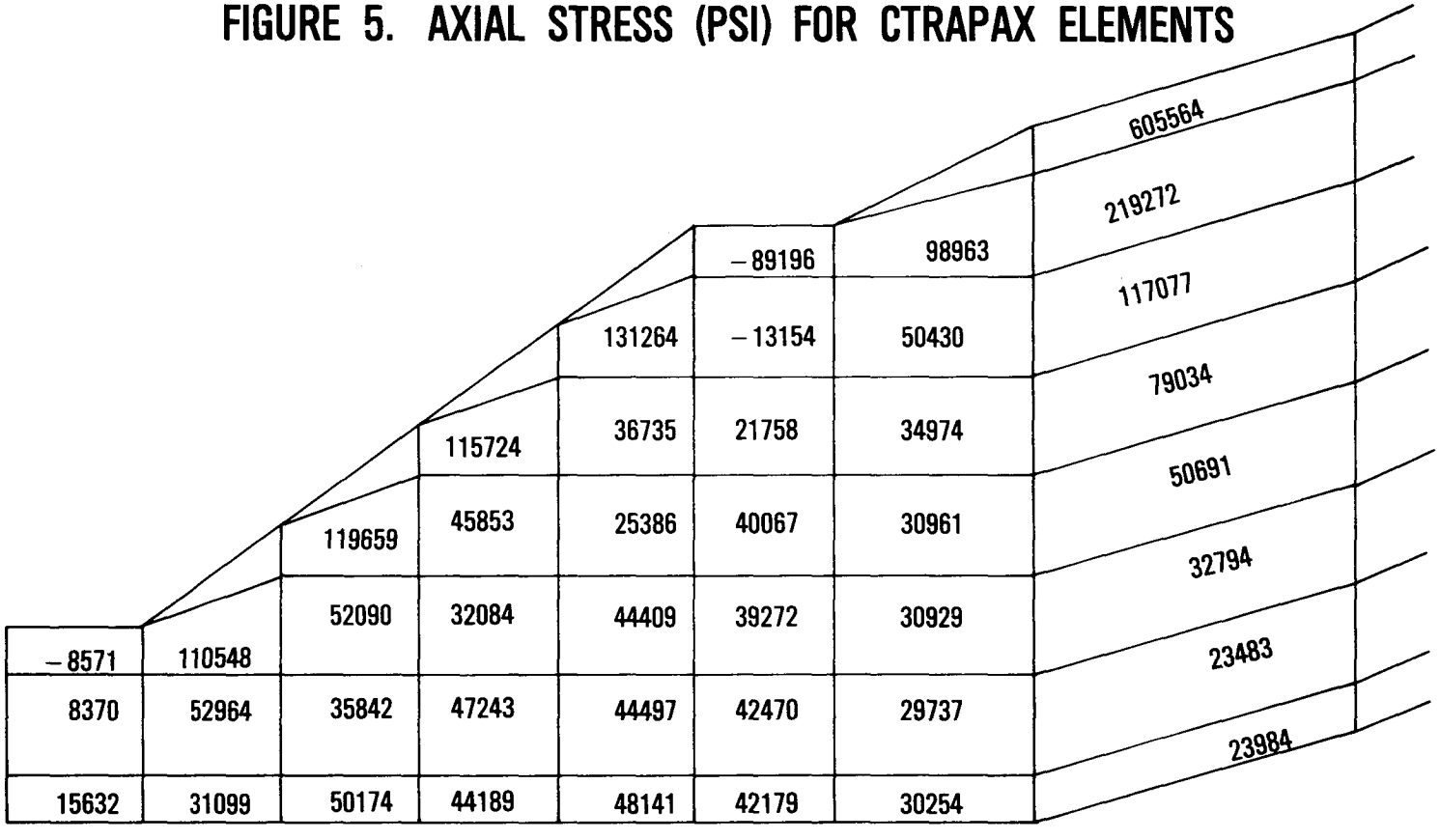

FIGURE 6. AXIAL STRESS (PSI) FOR CTRAPRG ELEMENTS

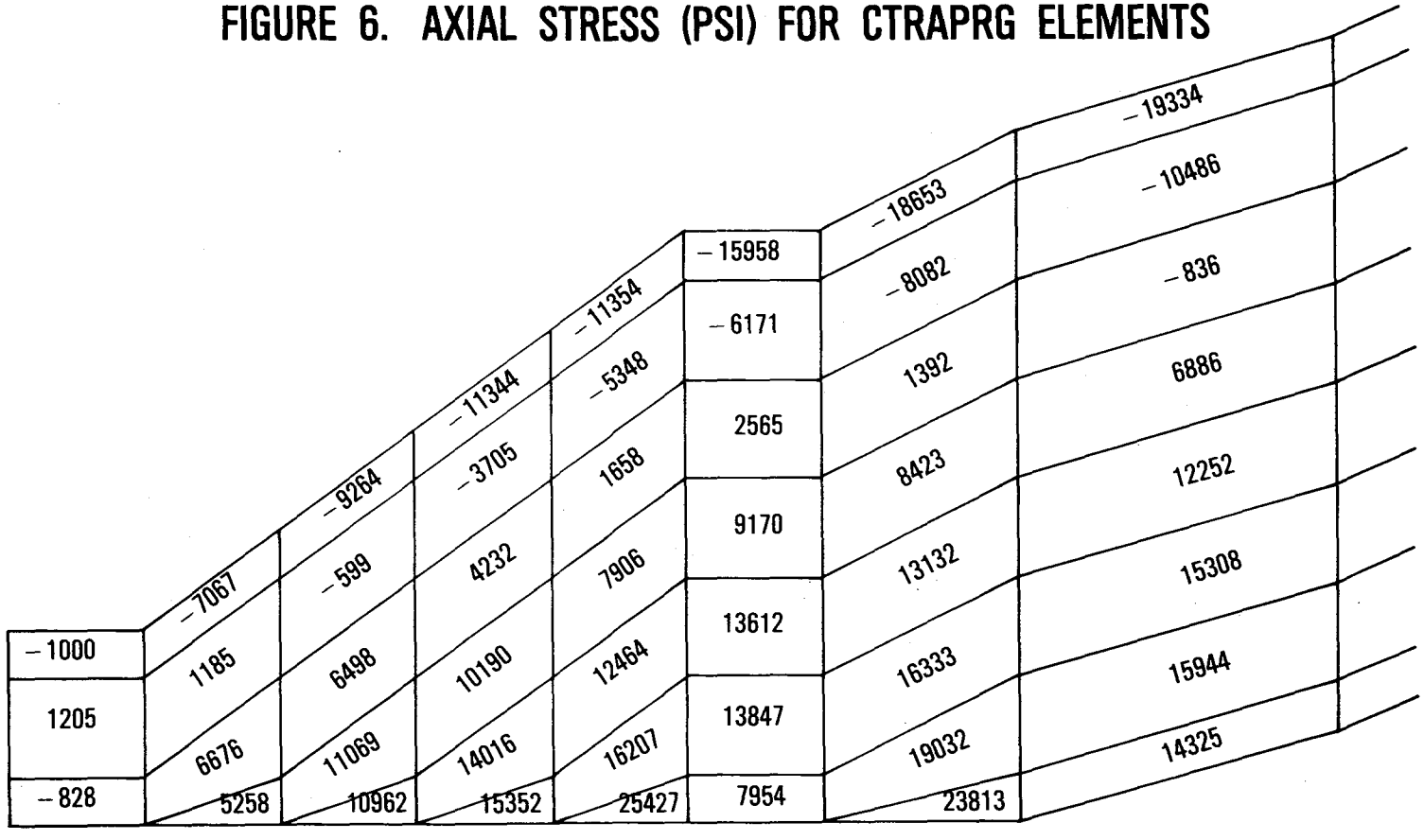

FIGURE 7. AXISYMMETRIC DISC MODEL

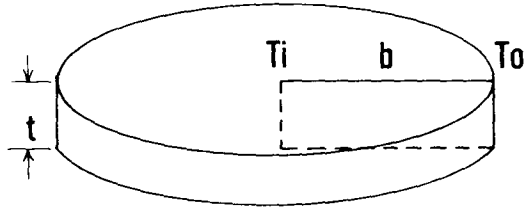

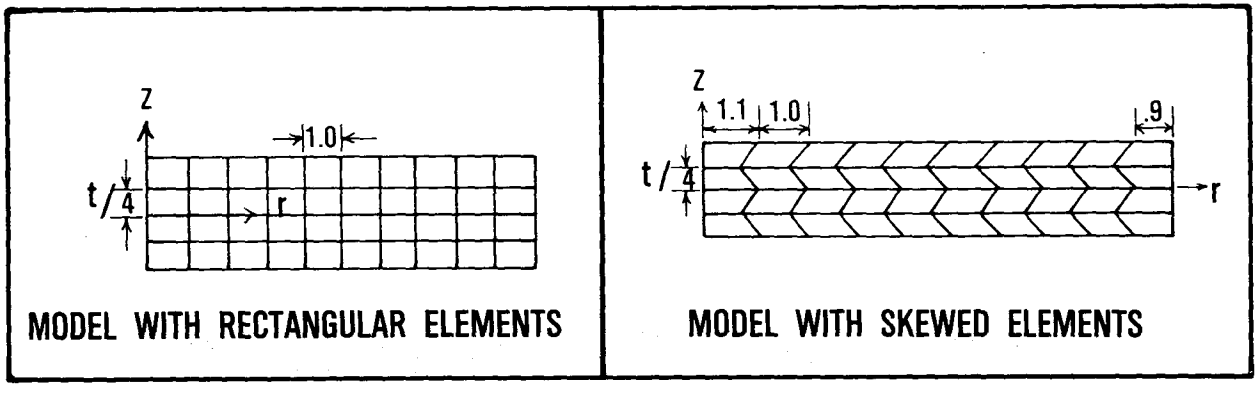

FIGURE 8. HOOP STRESS FOR SKEWED ELEMENTS (TEMPERATURE INDEPENDENT MATERIALS)

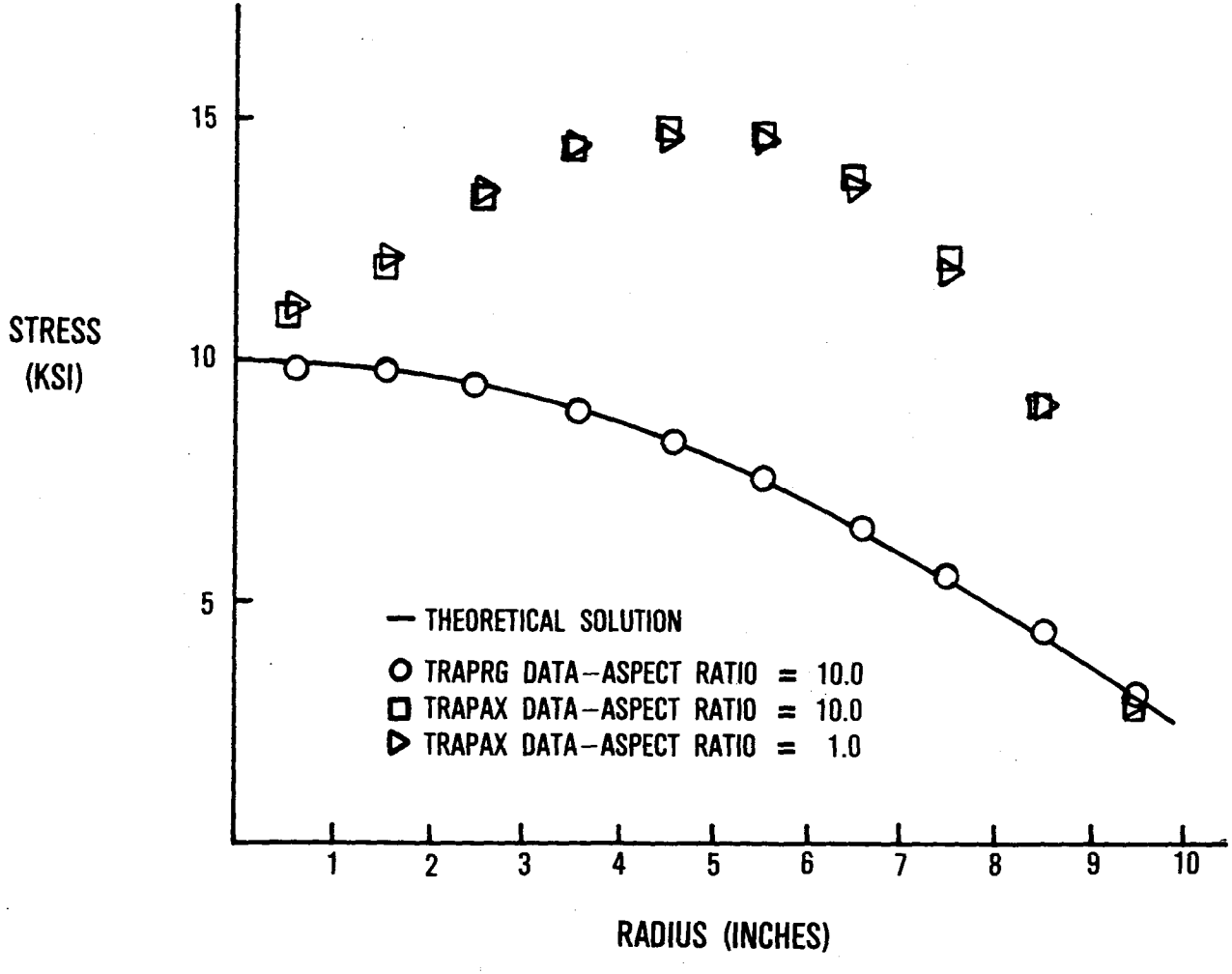

FIGURE 9. AXIAL STRESS FOR SKEWED ELEMENTS (TEMPERATURE INDEPENDENT MATERIAL)

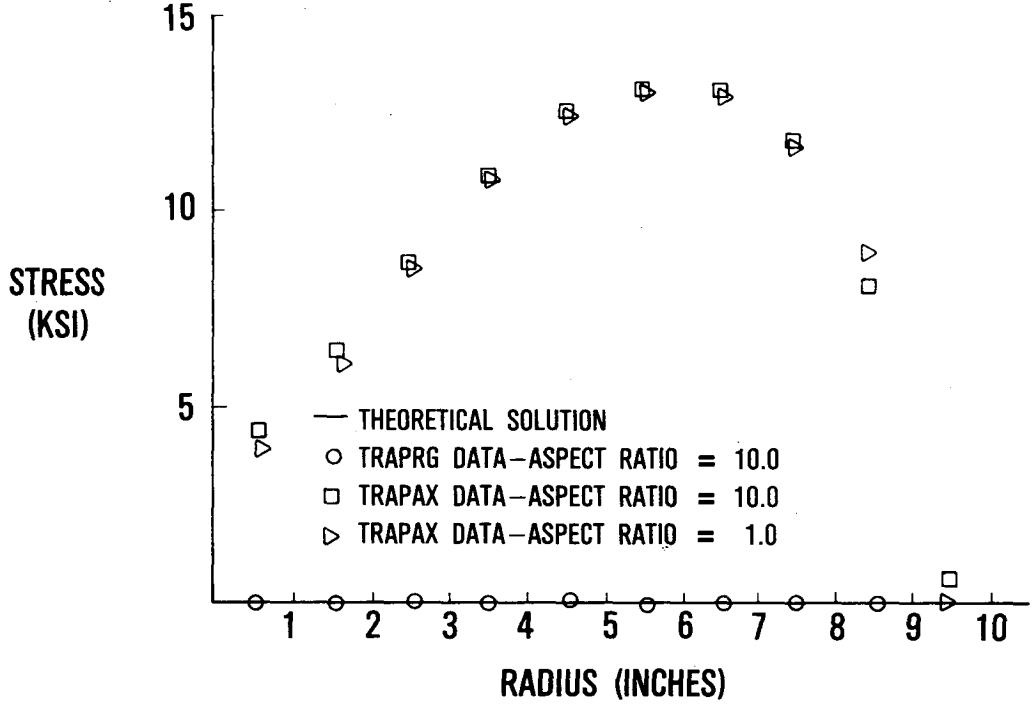

FIGURE 10. HOOP STRESS FOR SKEWED ELEMENTS (TEMPERATURE DEPENDENT MATERIAL)

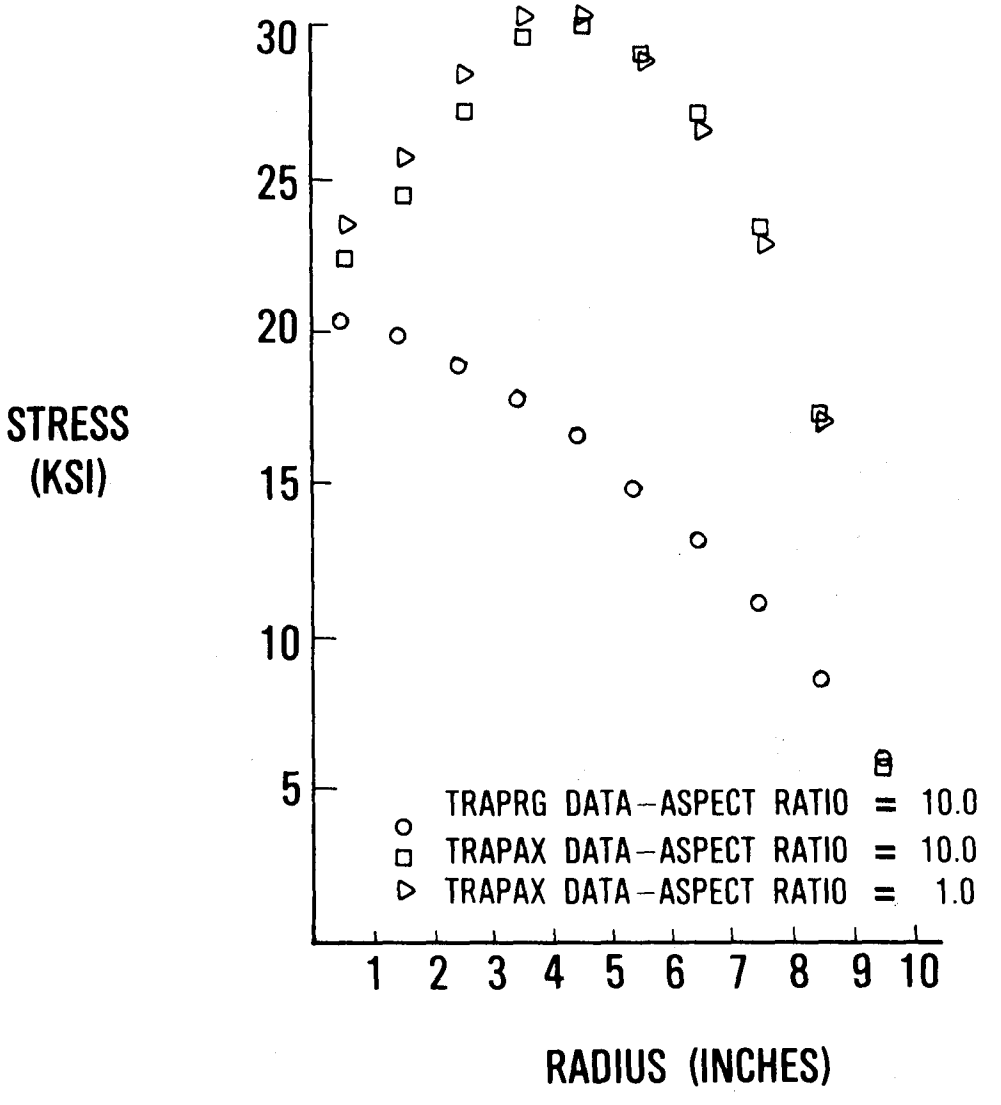

FIGURE 11. AXIAL STRESS FOR SKEWED ELEMENTS (TEMPERATURE DEPENDENT MATERIALS)

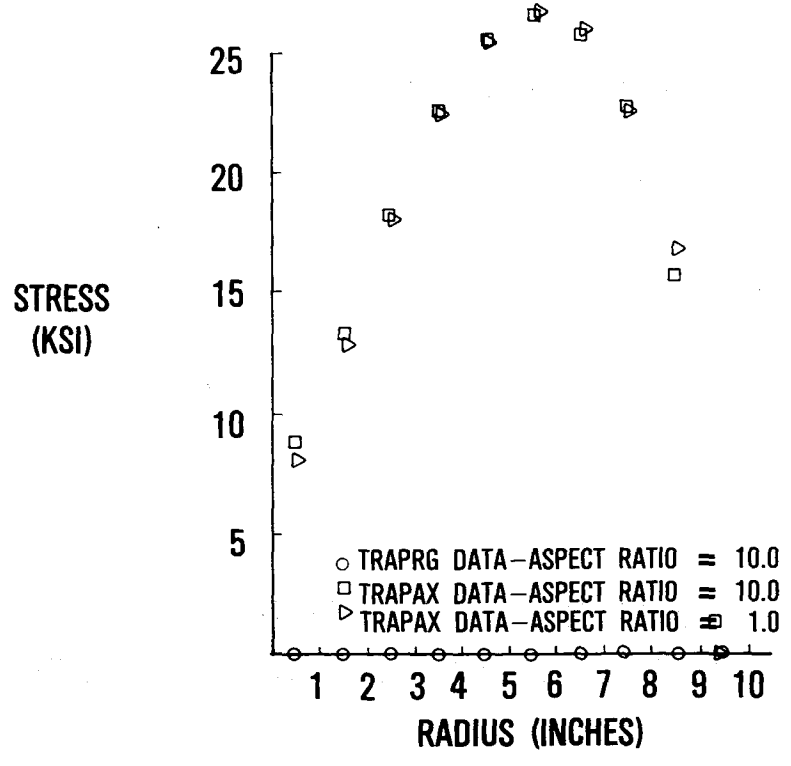

FIGURE 12. AXISYMMETRIC RING MODEL SUBJECTED TO ASYMMETRIC HEATING

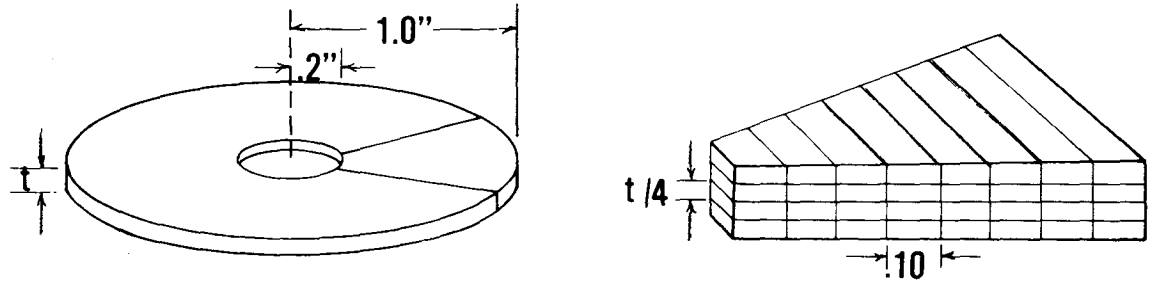

CIHEX WEDGE MODEL USED FOR CYCLIC SYMMETRY

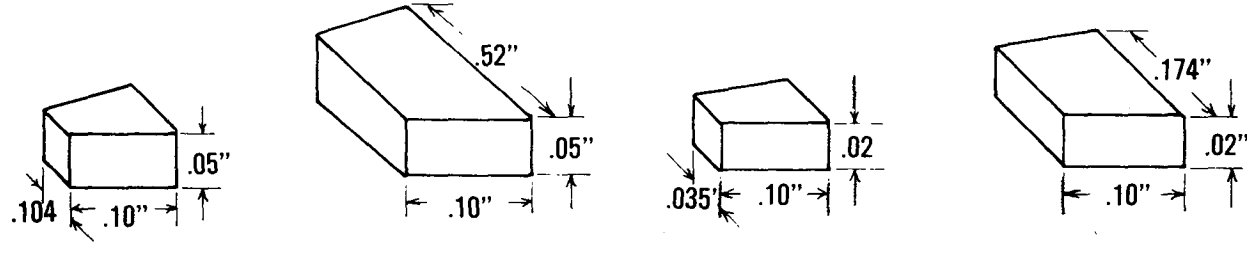

30° WEDGE-ASPECT RATIO RANGE
2/1 TO 10/1

10° WEDGE-ASPECT RATIO RANGE
5/1 TO 9/1

FIGURE 13. HOOP STRESS IN THE ASYMMETRICALLY HEATED RING (RADIUS = .25 INCHES)

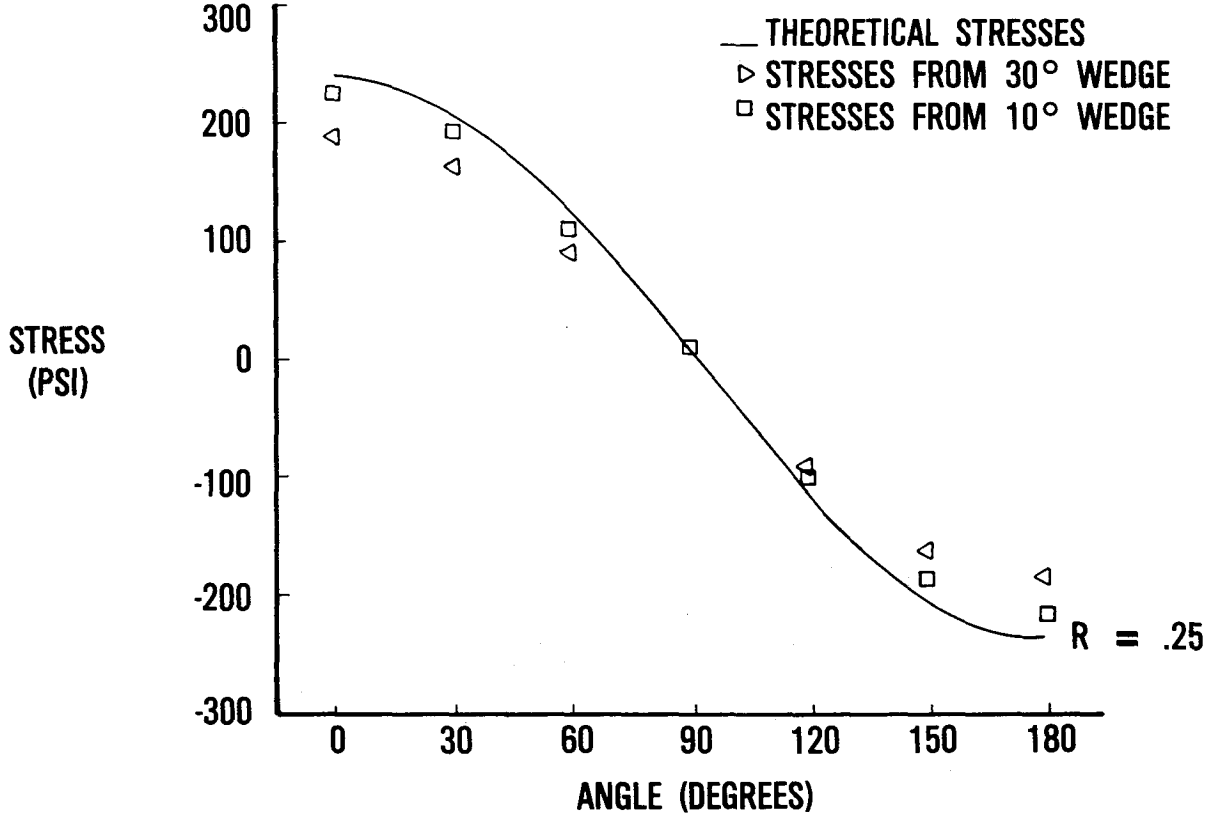

FIGURE 14. HOOP STRESS IN THE ASYMMETRICALLY HEATED RING (RADIUS = .55 INCHES)

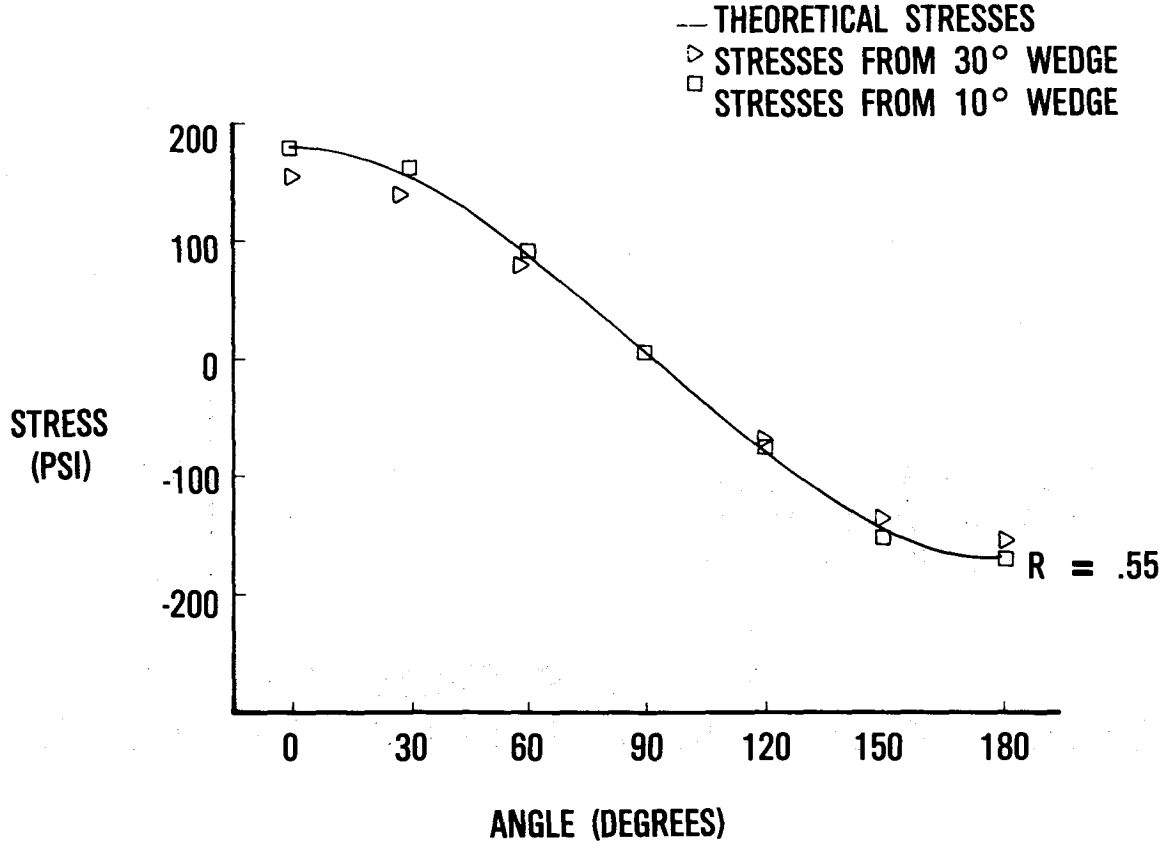

FIGURE 15. HOOP STRESS IN THE ASYMMETRICALLY HEATED RING (RADIUS = .95 INCHES)